Signature for heavy Majorana neutrinos in hadronic collisions

F. M. L. Almeida, Jr.,* Y. A. Coutinho,† and J. A. Martins Simões‡

Instituto de Física, Universidade Federal do Rio de Janeiro, RJ, Brazil

M. A. B. do Vale§

Centro Brasileiro de Pesquisas Físicas, Instituto de Física, Universidade Federal do Rio de Janeiro, RJ, Brazil

The production and decay of new possible heavy Majorana neutrinos are analyzed in hadronic collisions. New bounds on the mixing of these particles with standard neutrinos are estimated according to a fundamental representation suggested by grand unified models. A clear signature for these Majorana neutrinos is given by same-sign dileptons plus a charged weak vector boson in the final state. We discuss the experimental possibilities for the future Large Hadron Collider (LHC) at CERN.

PACS number(s): 12.60.−i, 14.60.St

I. INTRODUCTION

The increasing experimental evidence for neutrino oscillations seems to indicate that physics beyond the standard model may be in sight. The combined results from solar, atmospheric and laboratory neutrinos, if confirmed, require at least one new light neutrino [1]. In addition to this possible new fourth neutrino, theoretical models must give some explanation of the mass spectrum of neutrinos, as well as of the pattern of mixing angles. This is usually accomplished by variations of the seesaw mechanism, with new heavy neutral leptons. Many models that have being proposed recently could account for these properties but all of them need further experimental tests [2]. One particular point that still needs confirmation is the nature of the neutrino fields— Majorana or Dirac.

In this paper we analyze the production and decay of new heavy Majorana neutrinos in hadronic collisions. In order to understand the smallness of neutrino masses, the most likely mechanism includes at least one new heavy Majorana neutrino. These neutrinos could have their origin in many grand unified models such as in the fundamental 27-plet of E_6 or in left-right symmetric models. Here we consider the case of new heavy neutral singlets. In practically all these models we have new interactions, new fermions, and a large Higgs sector. As we have presently no evidence for new interactions, we will make the hypothesis that the new neutrino interactions are dominated by the standard Z and W weak gauge bosons. New Z' and W' are possible but they are known to have a small coupling with the standard fermions. Since these Majorana fermions can decay in both charged positive and negative leptons, they will give us very clear signatures. One interesting signature is given by the production of a pair of same-sign dileptons accompanied by a charged weak vec-

tor boson. This signature was already suggested in models with a new right weak boson [3] and composite Majorana neutrinos [4]. In a previous work [5] we have presented estimates for this process in a model with heavy Majorana neutrinos mixed with standard neutrinos. Here we generalize our results for the mixing of light and heavy neutrinos and present new bounds on mixing angles. As we will discuss in Sec. II, the mixing with new possible heavy singlets makes pair production of Majorana neutrinos suppressed relative to a single heavy Majorana production. We have calculated the general elementary process $q_i \bar{q}_j \rightarrow l^- l^- W^+$, with $l = e, \mu$, including finite-width effects, and discuss experimental cuts for the Large Hadron Collider (LHC) at CERN energies in Sec. III and give our conclusions in Sec. IV.

II. THE MODEL AND BOUNDS ON MIXING ANGLES

The key element in our analysis is the mixing between the standard light neutrinos and a new heavy one. Recent experimental searches at the $e^+ e^-$ collider LEPII at CERN imply that these new possible neutral states must have a mass above the standard Z mass [6]. This kind of mixing is different from the light-to-light mixing, which seems necessary in order to explain the standard neutrino properties in solar and atmospheric phenomena. We work in a scenario where each fermionic family is enlarged and the mixing occurs with neutrinos of the same generation. In the naive seesaw model, the mixing between light and heavy neutrinos is given by $\theta \simeq m_\nu / m_N$ and it is clearly out of any visible effect. However, there are many theoretical models which decouple the mixing from the mass relation [7]. The mechanism is very simple. In the general mass matrix including Dirac and Majorana fields one imposes some internal symmetry that makes the matrix singular. Then the mixing parameter has an arbitrary value, bounded only by its phenomenological consequences. We take this mixing to be described by a single parameter (for each generation), with the new heavy states appearing as isosinglets. The general Lagrangian of this kind of model is then given by

---

*Email address: marroqui@if.ufrj.br

†Email address: yara@if.ufrj.br

‡Email address: simoes@.if.ufrj.br

§Email address: aline@if.ufrj.br

$$\mathcal{L} = \sum_{l=e,\mu,\tau} \left\{ -\frac{g}{2\sqrt{2}} [\bar{\nu}_l \gamma^\mu (1-\gamma^5) l \cos\theta_l + \bar{N}_l \gamma^\mu \right.$$

$$\times (1-\gamma^5) l \sin\theta_l] W_\mu - \frac{g}{2\cos\theta_W} \left[\bar{\nu}_l \gamma^\mu (g_{V_l} - g_{A_l}\gamma^5) \nu_l \right.$$

$$+ \frac{1}{2}\cos\theta_l \sin\theta_l \bar{N}_l \gamma^\mu (1-\gamma^5) \nu_l + \frac{1}{2}\sin^2\theta_l \bar{N}_l \gamma^\mu$$

$$\left. \times (1-\gamma^5) N_l \right] Z_\mu + \text{H.c.} \right\}, \tag{2.1}$$

where

$$g_{V_l} = g_V^{SM} - \frac{1}{2}\sin^2\theta_l, \tag{}$$

$$g_{A_l} = g_A^{SM} - \frac{1}{2}\sin^2\theta_l. \tag{2.2}$$

We have considered only the first and second families, since electrons and muons are directly observable particles. The $\tau^\pm \tau^\pm$ dileptons are also possible, but the associated Majorana neutrino can be heavier than the corresponding to the other families. Besides that, the final state for tau leptonic decays has to be reconstructed with undetected neutrinos.

The W and Z couplings to standard leptons are well known to agree with the experimental data on low-energy lepton-hadron scattering, with the high-precision Z data at CERN and SLAC, as well as with all the charged current experiments. This implies that the mixing angle θ_l must be small. It is also well known that the present experimental data require standard model quantum corrections in order to compare theory and data. With this in mind, we take the changes in the physical observables due to new neutrino mixing to be small contributions to the standard model theoretical results, including first order corrections. With α_{em} and M_Z as fundamental input parameters, the mixing indicated in Eq. (2.1) above will imply corrections to the effective μ-decay constant G_μ, charged coupling lepton universality, Cabbibo-Kobayashi-Maskawa unitarity, and neutral current interactions. The most stringent bounds on θ_e come from the effective coupling of the Z to the electron neutrino [6] $g_{expt}^{ve} = 0.528 \pm 0.085$ and $\Gamma_{expt}^{inv}(Z) = 500.1 \pm 1.8$ MeV, to be compared with the standard model predictions $g_{SM} = 0.5042$ and $\Gamma_{SM}^{inv}(Z) = 501.7 \pm 0.2$ MeV. For the muon neutrino coupling with the Z boson, the Particle Data Group quotes $g_{expt}^{\nu\mu} = 0.502 \pm 0.017$. After a global fit to the data we have obtained, at 95% confidence level, the upper bounds

$$\sin^2\theta_e < 0.0052, \tag{2.3}$$

$$\sin^2\theta_\mu < 0.0001. \tag{2.4}$$

These bounds are more restrictive than an earlier analysis [8]. Since the muon bound is much stronger, the dimuon channel will be much smaller than the dielectron channel for
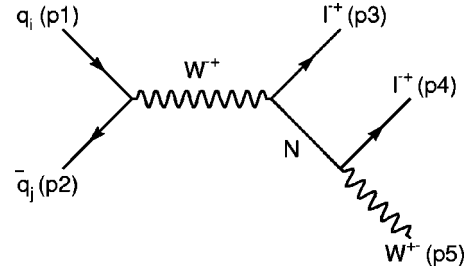

FIG. 1. Feynman diagram for the elementary process $q_i \bar{q}_j \rightarrow l^- l^- W^+$.

the LHC at CERN. We are left then with the possibility of detecting the Majorana contribution in the $e^\pm e^\pm$ channel.

With these bounds we can compare the total cross section for single and heavy pair neutrino production. The interaction shown in Eq. (2.1) implies that heavy pair production is suppressed if compared with single production of a heavy neutrino, as was shown in [5].

III. RESULTS

The fundamental production mechanism is given by quark-antiquark annihilation into a W followed by the single Majorana production and decay, as shown in Fig. 1. At the LHC at CERN center of mass energies ($\sqrt{s} = 14$ TeV) other contributions such as gluon fusion will give a small contribution. We have also checked the contribution from WW fusion which turns out to be small. Let us now discuss the main characteristics of the final state identification. Experimentaly each charged lepton can be isolated into a cone, with no accompanying hadrons, in order to eliminate possible misidentification from hadron decays. The dominant final state $W \rightarrow$ jets has a sharp kinematical identification in the invariant mass. The leptonic $W \rightarrow l\nu_l$ decay can be identified by the total p_T balance with a reconstructed neutrino. The proposed detectors [9] for the LHC at CERN energies are planned to have a good leptonic and hadronic resolution, as well as a wide rapidity coverage. We have estimated the total cross section for $pp \rightarrow l^\pm l^\pm W^\mp X$, applying conservative cuts on the final state. For the charged leptons we considered $p_{Tl} > 5$ GeV and a pseudorapidity $|\eta| < 2.5$. For the charged weak boson the cuts $|\eta| < 2.5$ and $p_{TW} > 15$ GeV were done. For the upper bound $\sin^2\theta_e = 0.0052$ our results are shown in Fig. 2. The analytic expression for the elementary process $q_i \bar{q}_j \rightarrow l^- l^- W^+$ is given in the Appendix. For the proton structure functions we have employed the MRS[G] set [10].

The standard model background comes mainly from top production and decay via the chain $t \rightarrow b \rightarrow c \quad l\nu_l$. It is well known [11] that prompt lepton background from heavy quark decay can be suppressed by a suitable isolation criteria on transverse energy and momentum. This procedure was applied in an earlier analysis [12] of Majorana neutrino production. We employed a cut of $p_T = 80$ GeV on the softer lepton coming from the standard model background. Since our estimate of mixing angles is more restrictive than previous values, the signal for Majorana neutrino production will be suppressed. An alternative to enhance the signal is to
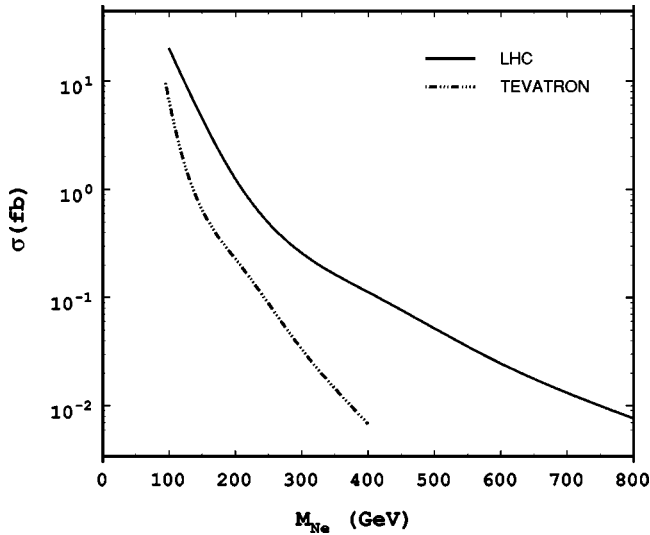
FIG. 2. Total cross section versus M_{N_e} for LHC at CERN and Tevatron at Fermilab energies.

employ a very distinctive characteristic between the signal and the standard model background: whereas in the Majorana neutrino production we have no undetected particles in the final state, for the heavy quark background we have two undetected neutrinos in the final state. As a consequence there is no missing transverse momentum, $\not{p}_T$, for the signal and for the background there is an average [12] $\not{p}_T \simeq 50$ GeV. A recent analysis [13] of detector possibilities at LHC energies indicates that an error in the missing transverse energy in the 10–20 GeV region is expected. The other kinematical difference between signal and background

is given by the total hadronic invariant mass in the final state. In the heavy lepton production we have the associated production of a single W boson, with a corresponding peak at the W mass. The standard model background has a very different hadronic mass distribution.

We show in Fig. 3 the correlation for the hadronic invariant mass versus final state missing energy variables. We have applied a cut on the transverse momentum of the least energetic lepton of $p_T > 35$ GeV. Both the signal and background events were hadronized according to PYTHIA [14]. The box in Fig. 3 shows the kinematical region of the expected signal events. We have considered a heavy Majorana neutrino with mass of 200 GeV. From Fig. 2 for a total cross section of 1 fb and for an expected luminosity of 100 fb^{-1} at LHC we have a total number of 100 events for the signal. For an invariant hadronic mass in the 60–85 GeV region, a total missing energy less than 12.5 GeV, and the most energetic charged lepton transverse momentum greater than 35 GeV, we still have 62 events from the signal, whereas for the standard model background we have only 8 remaining events. With these cuts, we estimate the ratio $s/\sqrt{s+b}$, where s and b are the signal and background number of events, to be 7.4. This clearly shows the advantages of applying the above procedure for the cuts. For higher neutrino masses the total cross section fall requires more stringent cuts on the suggested variables. In this case other kinematical restrictions may be useful. The standard model background can still be reduced one order of magnitude by requiring only two hadronic jets in the final state and by increasing the transverse momentum cut on the charged leptons. In Fig. 4 we display the transverse momentum of the final leptons for some values of the Majorana neutrino mass.
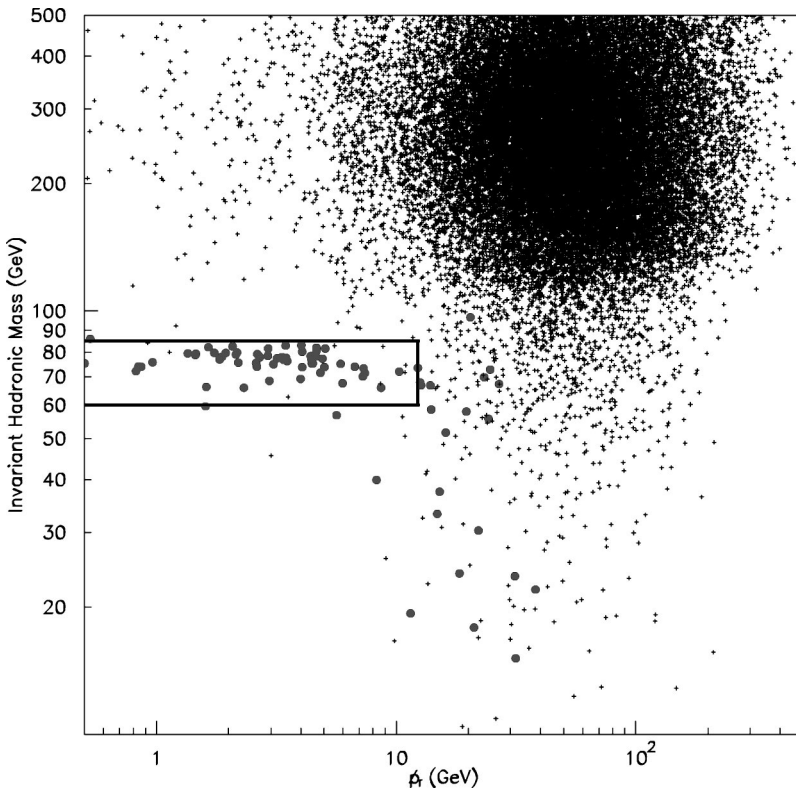

FIG. 3. Invariant hadronic mass versus total missing momentum for the standard model (crosses) and signal (bullets) events with $M_{N_e} = 200$ GeV.
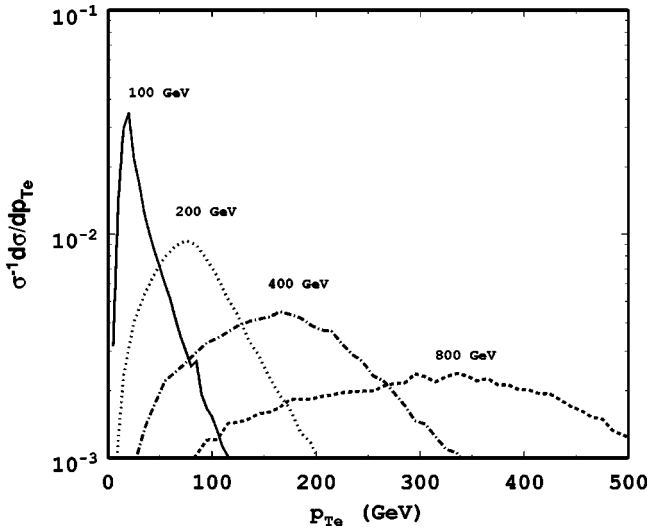
FIG. 4. Normalized final lepton transverse momentum distributions for $M_{N_e} = 100$, 200, 400, and 800 GeV for LHC at 14 TeV.

For masses in the 100–200 GeV region, a high-p_T cut of 80 GeV strongly reduces the signal but for higher masses there are practically no changes. For example, for $m_N = 200$ GeV the cross section shown in Fig. 2 (calculated for $p_T = 5$ GeV) is reduced by a factor of 3 if we increase the p_T cut to 80 GeV. A similar procedure for $m_N = 400$ GeV reduces the signal by 20% and for $m_N = 800$ GeV there is almost no change. From the expected luminosity at LHC, we took $m_N = 800$ GeV as a superior limit in the neutrino mass spectrum. For this extreme value of m_N only one event is expected, with no further cuts, for a luminosity of 100 fb^{-1}. This is a poor result from the statistical point of view, but this signal has a very interesting characteristic. In Fig. 5 we show the distribution for the angle between the two final leptons in the laboratory frame. We can see that for heavier masses region the two leptons tend to be emitted back to back. We can then safely expect that the background can be
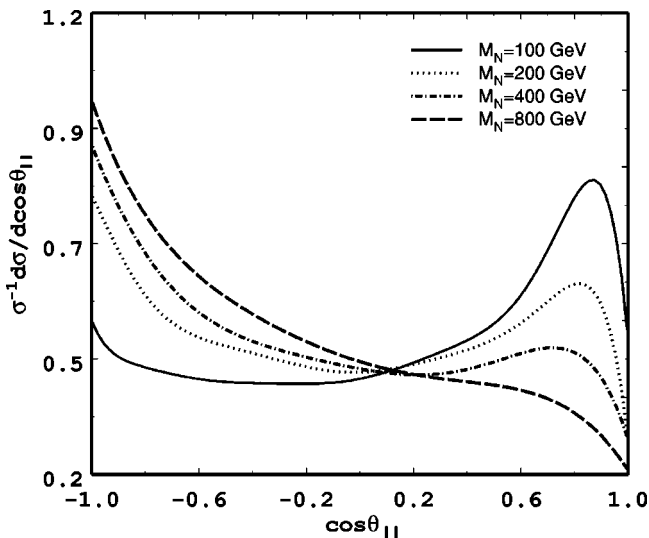

FIG. 5. Normalized dilepton angular distribution $\cos \theta_{ll}$ for $M_{N_e} = 100$, 200, 400, and 800 GeV for LHC at 14 TeV.
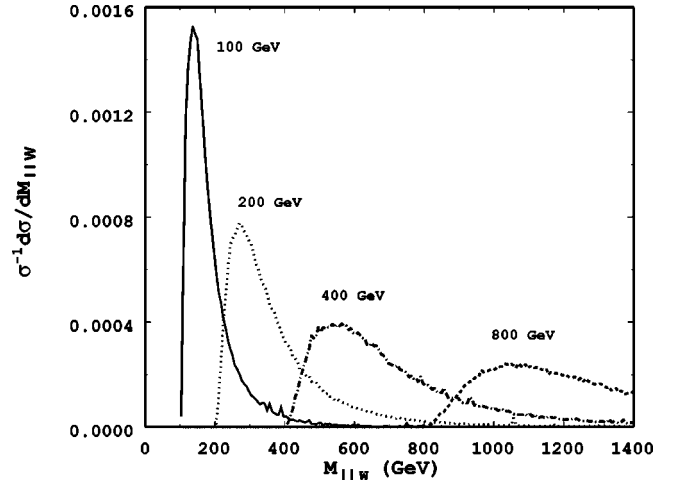

FIG. 6. Normalized invariant mass distribution M_{llW} for $M_{N_e} = 100$, 200, 400, and 800 GeV for LHC at 14 TeV.

reduced by the simple requirement of low missing transverse energy in the final state, combined with the hadronic invariant mass peaked around the W masss.

We have also estimated the cross section for the Tevatron upgrade center of mass energies ($\sqrt{s} = 2$ TeV) at Fermilab with a luminosity of 1000 pb^{-1}. For a new possible heavy Majorana neutrino with a mass of 95 GeV we have ten events, applying the following cuts: for the leptons and the charged weak bosons we used $|\eta| < 2.0$ and $E_l > 10$ GeV. We use the bound on the neutrino mixing parameter $\sin^2 \theta_e = 0.0052$. The number of events falls to 1 for a mass value of 140 GeV, applying the same cuts and mixing angle as before.

We now turn our attention to the other kinematical characteristics of the final state particles. The final W can be identified in the channel $W \rightarrow$ jets or in the leptonic channel. The distribution for the total invariant mass $M_{llW}^2 = (p_l + p_l + p_W)^2$ is shown in Fig. 6. A better identification of the heavy neutrino mass is given by the invariant mass M_{lW}.
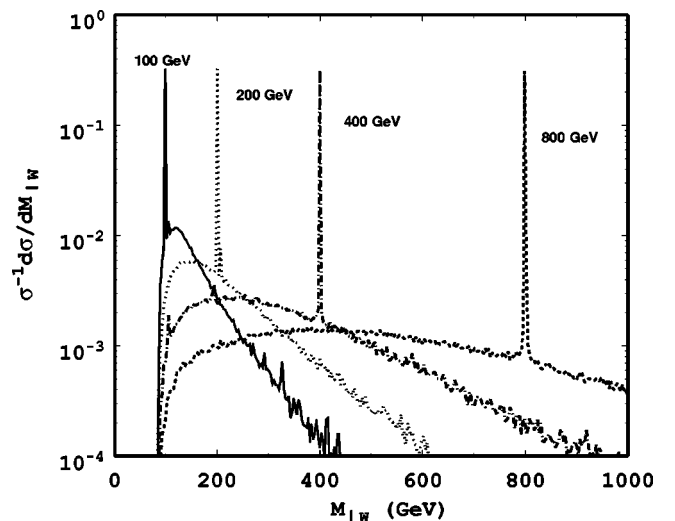

FIG. 7. Normalized invariant mass distribution M_{lW} for $M_{N_e} = 100$, 200, 400, and 800 GeV for LHC at 14 TeV.
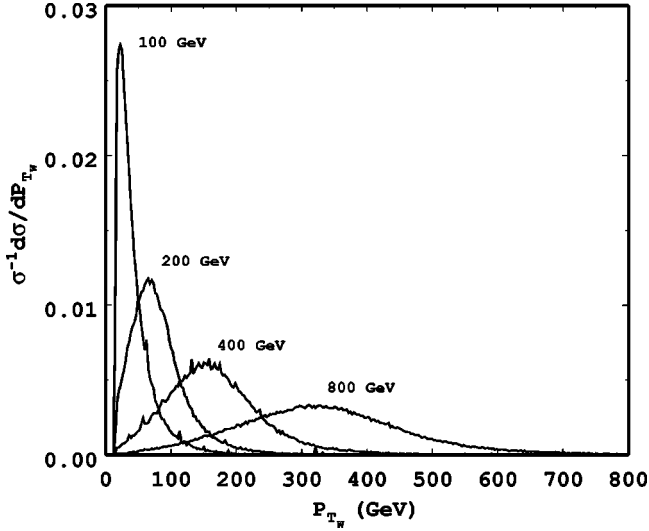
FIG. 8. Normalized W transverse momentum distributions for $M_{N_e} = 100$, 200, 400, and 800 GeV for LHC at 14 TeV.

Since we have two indistinguishable particles in the final state, we must take the variable $M^2_{lW} = (p_l + p_W)^2$ including all the combinations between the two leptons and the W. This distribution presents a well-defined peak at the Majorana mass, as shown in Fig. 7. The total width for a 100 GeV neutrino is 0.00065 GeV and for a 800 GeV neutrino is 0.058 GeV. As mentioned before, another variable that can be useful in the identification of the final state particles is the angle between the two charged leptons. The distribution for $\cos\theta_{ll}$ is shown in Fig. 5, calculated in the hadronic center of mass frame. For lower M_N mass (100 GeV) they have a larger

probability of being parallel. This is the case also for the Tevatron at Fermilab with $M_N \approx 90$–140 GeV. For higher masses (800 GeV), they show a preference for being emitted back to back. Finally we show in Fig. 8 the p_{TW} distribution for the final W. This is an important point in order to eliminate any possible standard model background. For lower neutrino mass a cut not greater than 30 GeV must be done in order not to lose the signal. For higher masses the p_{TW} cut can be safely higher.

IV. CONCLUSIONS

We have presented an analysis of the possibility of detecting new heavy Majorana neutrinos through same-sign dileptons and W detection. The agreement between the standard model predictions and the present experimental data implies that the mixing angle between heavy and light states must be small. For the second family, the upper bound for the mixing angle implies that the dimuon final state must be suppressed by one order of magnitude relative to the dielectron channel. For the Tevatron upgrade at $\sqrt{s} = 2$ TeV, we found a detectable signal in a small region in the heavy neutrino mass. For the next LHC the situation is more favorable, allowing an investigation for new heavy Majorana neutrinos in the range 100–800 GeV. The signal to background ratio can be increased by a combined cut on the invariant hadronic mass and low missing energy in the final state instead of a single high-p_T cut.

APPENDIX

The elementary cross section for the process $q_i\bar{q}_j \to l^- l^- W^+$ $(i,j = u,d,s,c)$, can be written as [15]

$$d\hat{\sigma}_{ij} = \Delta_{ij}\{D - C\}dLips, \tag{A1}$$

where

$$\Delta_{ij} = \frac{g^6 U^2_{ij}\sin^4\theta_l M^2_{Nl}}{6}, \tag{A2}$$

$$D = \frac{2p_{14}p_{23}}{Pr(-p_1 - p_2, M_W, \Gamma_W)^2 Pr(p_4 + p_5, M_{Nl}, \Gamma_{Nl})^2}, \tag{A3}$$

$$C = \frac{p_{24}p_{13} + p_{14}p_{23} + \left(-p_{14} - p_{23} - p_{24} - p_{13} + p_{12} - \frac{1}{2}M^2_W\right)p_{12}}{Pr(-p_1 - p_2, M_W, \Gamma_W)^2 Pr(p_4 + p_5, M_{Nl}, \Gamma_{Nl})Pr(p_3 + p_5, M_{Nl}, \Gamma_{Nl})}. \tag{A4}$$

The propagator effects are included via the function

$$Pr(P, M_k, \Gamma_k) = (P^2 - M^2_k) - i(\Gamma_k M_k), \quad k = W, N_l, \tag{A5}$$

with $l = e, \mu$.

The four-momenta for the quark, antiquark, primary lepton, secondary lepton, and boson are, respectively, p_1, p_2, p_3, p_4, and p_5. To simplify our notation we have called the product between two four-momenta as $p_{mn} = p_m \cdot p_n$. Finally U_{ij} is the standard quark mixing matrix.

[1] K. Zuber, Phys. Rep. **305**, 295 (1998).

[2] J. Ellis, hep-ph/9907458; G. Altarelli, hep-ph/9809532.

[3] D.A. Dicus, D.D. Karatas, and D.P. Roy, Phys. Rev. D **44**, 2033 (1991); A. Datta, M. Guchait, and D.P. Roy, *ibid.* **47**, 961 (1993).

[4] O. Panella, C. Carimalo, and Y.N. Srivastava, Phys. Rev. D **62**, 015013 (2000).

[5] F.M.L. Almeida, Jr., Y.A. Coutinho, J.A. Martins Simões, P.P. Queiróz Filho, and C.M. Porto, Phys. Lett. B **400**, 331 (1997).

[6] Particle Data Group, C. Caso *et al.*, Eur. Phys. J. C **3**, 1 (1998).

[7] C. Jarlskog, Phys. Lett. B **241**, 579 (1990); D. Tommasini, G. Barenboim, J. Bernabéu, and C. Jarslkog, Nucl. Phys. **B444**, 451 (1994); W. Buchmüller, C. Creub, and P. Minkovski, Phys. Lett. B **267**, 355 (1991).

[8] E. Nardi, E. Roulet, and D. Tommasini, Phys. Lett. B **327**, 319 (1994); P. Bamert, C.P. Burgess, and I. Maksymyk, Phys. Lett. B **267**, 282 (1995).

[9] ATLAS Collaboration, Technical Proposal No. CERN/LHCC/ 94-43.

[10] A.D. Martin, R.G. Roberts, and W.J. Stirling, Phys. Lett. B **354**, 155 (1995).

[11] N.K. Mondal and D.P. Roy, Phys. Rev. D **49**, 183 (1994); R.M. Godbole, S. Pakvasa, and D.P. Roy, Phys. Rev. Lett. **50**, 1539 (1983); V. Barger and R.N. Phillips, Phys. Rev. D **28**, 145 (1983).

[12] A. Datta, M. Guchait, and A. Pilaftsis, Phys. Rev. D **50**, 3195 (1994).

[13] ATLAS Collaboration, Detector and Physics Performances Technical Design Report No. ATLAS TDR 14, CERN/LHCC 99-14, Vol. I, Sec. 2.5.9.

[14] T. Sjöstrand, Comput. Phys. Commun. **82**, 74 (1994).

[15] A. Pukhov, E. Boss, M. Dubinin, V. Edneral, V. Ilyin, D. Kovalenko, A. Krykov, V. Savrin, S. Shichanin, and A. Semenov, ''CompHEP''—a package for evaluation of Feynman diagrams and integration over multi-particle phase space, Report No. INP MSU 98-41/542, hep-ph/9908288.